Chaos, Solitons and Fractals 84 (2016) 23–30

Contents lists available at ScienceDirect

Chaos, Solitons and Fractals

Nonlinear Science, and Nonequilibrium and Complex Phenomena

journal homepage: www.elsevier.com/locate/chaos

Emergence of a multilayer structure in adaptive networks of phase oscillators

V.V. Makarov[a,b], A.A. Koronovskii[a,b], V.A. Maksimenko[a,b], A.E. Hramov[b,a], O.I. Moskalenko[a,b,*], J.M. Buldú[c,d], S. Boccaletti[e,f]

[a] Faculty of Nonlinear Processes, Saratov State University, Astrakhanskaya 83, Saratov 410012, Russia
[b] REC 'Nonlinear Dynamics of Complex Systems', Saratov State Technical University, Politechnicheskaja 77, Saratov 410054, Russia
[c] Laboratory of Biological Networks, Center for Biomedical Technology, 28923 Pozuelo de Alarcón, Spain
[d] Complex Systems Group & GISC, URJC, 28933 Móstoles, Spain
[e] CNR – Institute of Complex Systems, Via Madonna del Prato, 10, 50019 Sesto Fiorentino (FI), Italy
[f] The Italian Embassy in Tel Aviv, Trade Tower, 25, Hamered St., 68125 Tel Aviv, Israel

ARTICLE INFO

Article history:
Received 22 September 2015
Accepted 17 December 2015
Available online 15 January 2016

PACS:
05.45.Xt
89.75.Hc

Keywords:
Multilayer networks
Homophily
Homeostasis
Kuramoto oscillators
Synchronization
Cluster formation

ABSTRACT

We report on self-organization of adaptive networks, where topology and dynamics evolve in accordance to a competition between homophilic and homeostatic mechanisms, and where links are associated to a vector of weights. Under an appropriate balance between the intra- and inter- layer coupling strengths, we show that a multilayer structure emerges due to the adaptive evolution, resulting in different link weights at each layer, i.e. different components of the weights' vector. In parallel, synchronized clusters at each layer are formed, which may overlap or not, depending on the values of the coupling strengths. Only when intra- and inter- layer coupling strengths are high enough, all layers reach identical final topologies, collapsing the system into, in fact, a monolayer network. The relationships between such steady state topologies and a set of dynamical network's properties are discussed.

Coupled biological and chemical systems, social groups and interacting animal species, the Internet and the World Wide Web, the brain and the stock markets are just a few examples of systems composed of a huge number of highly interconnected dynamical components. The modern approach to capture the global properties of such systems is to model them as graphs [1–4], where nodes represent the basic units, and links stand for the interactions between them, forming a specific connectivity pattern which defines the so-called network's topology. Despite their intrinsic differences, a set of surprising common properties, such as a power law scaling in the network connectivity and the coexistence of modules observed at the mesoscopic scale, has been revealed in real-world network (RWN) [5]. The spontaneous emergence of these topological features has been recently explained as a consequence of a self-organization process involving structure-dynamics adaptation of two fundamental mechanisms [6,7]. The first one corresponds to the trend of reinforcing those interactions with other correlated units in the network, which is a well established process known as *homophily* in the case of social systems [8] and Hebbian learning in the field of neuroscience [9]. The second process results instead from the limitation of the associative capacity, which preserves

* Corresponding author at: Faculty of Nonlinear Processes, Saratov State University, Astrakhanskaya 83, Saratov 410012, Russia. Tel.: +78 452512111; fax: +78 452523864.
E-mail address: o.i.moskalenko@gmail.com, moskalenko@nonlin.sgu.ru, mos425@mail.ru (O.I. Moskalenko).

http://dx.doi.org/10.1016/j.chaos.2015.12.022
0960-0779/

the value of the inputs/outputs received by each unit. This mechanism is known as *homeostasis* [10] in neuroscience, while in social systems it is related to the so-called Dunbar's number [11], which explains the existence of a maximum number of interactions for an individual.

Up until recently, attention was almost exclusively concentrated on networked systems where all components were treated on an equivalent footing, while neglecting all the extra information about the temporal- or context-related properties of RWNs' interactions. Only in the last years, and taking advantage of an enhanced resolution in real data sets, the interest switched to properly frame the *multilayer* character of RWNs, by considering them as networks made of diverse relationships (layers) between their constituents [12,13]. The analysis of multilayer networks started with a reformulation of classical topological parameters, such as the shortest path length, clustering coefficient, centrality or robustness of the nodes [14–17]. From the dynamical perspective, the multilayer formulation has been applied both to networks whose layers coexist or alternate in time [13]. In both cases, the multilayer formulation allows to identify synchronization regions that arise as a consequence of the interplay between the layers' topologies [18–20], as well as to define new types of synchronization based on the coordination between layers [21].

In this paper, we focus on how the competition between homophily and homeostasis can actually lead to self-organization of ensembles of oscillators into a multilayer network structure. To this purpose, we will consider a generic adaptive network of phase oscillators, and report the way a multilayer structure of interactions emerges and is maintained when the weights of the network's connections evolve according to the dynamical properties of the nodes and, conversely, how the evolution of the network topology influences the dynamics of the nodes and their ability to synchronize. Particularly, we make use of an extension of the classical Kuramoto model [22] as a paradigmatic phase oscillator able to describe the dynamics of a series of physical, biological, technological and social systems [23,24]. This way we are able to investigate the interplay between the generic dynamics of phase oscillators and the evolution of the structure where the dynamical units are constrained to interact.

Our starting point is, then, an ensemble of N oscillators whose dynamics evolves in time. Each oscillator i ($i = 1, \ldots, N$) has a natural frequency ω_i, and, in order to encompass the most general case, it is described by a *phasor* $\vec{\phi}_i$, i.e. a vector of M components ϕ_i^l ($l = 1, \ldots, M$) which actually stand for its instantaneous, time dependent, phases in each of the M layers of the multilayer network on which the oscillator interacts with the rest of the ensemble. For the sake of simplicity, we assume a Kuramoto-like evolution for the phase $\phi_i^l(t)$ on each layer $l = 1, \ldots, M$. Our choice is motivated by the fact that the interaction of Kuramoto oscillators is a paradigm of synchronization in nonlinear science [22], and actually represents (though in its simplicity) a rather elegant way to encompass synchronous phenomena occurring in many biological (such as circadian clocks), technological (electrical generators), and social systems (opinion formation). Furthermore, for each oscillator, we model layer-layer interactions by an additional coupling term accounting for the rigidity of the phasor, i.e. implying all-to-all interactions between the different components of the vector $\vec{\phi}_i$. The resulting evolution of the phasors is given by

$$\dot{\phi}_i^l(t) = \omega_i + \sigma_1 \sum_{j \neq i} w_{ij}^l(t) \sin(\phi_j^l - \phi_i^l) + \sigma_2 \sum_{j \neq l} \sin(\phi_i^j - \phi_i^l). \quad (1)$$

Here, $\{\omega_i\}$ is a set of randomly assigned natural frequencies distributed uniformly in $[-\pi, \pi]$ (note that the natural frequency ω_i of ith oscillator is the same for all M layers of the network), and σ_1 and σ_2 are the intra- and inter-layer coupling strengths, respectively.

This way, the exchange of information of the dynamical state of each layer relies on the interaction of the phases within the same oscillator i, which is controlled by the inter-layer coupling σ_2.

On the other hand, $w_{ij}^l(t)$ is the weight of the connection between elements i and j on layer l and it is allowed to evolve in time, e.g. layers are allowed to reorganize internally. On each layer l, for each oscillator i and at each time t, the set of connection weights $\{w_{ij}^l\}$ satisfies the condition

$$\sum_{j \neq i}^{N} w_{ij}^l = 1. \quad (2)$$

In other words, we consider the case for which, in Eq. (2), the input strength received by each unit i within each layer is constant, as in homeostatic processes [21].

In parallel with the node dynamics given by Eq. (1), the weights of the links are also evolving following differential equations that reflect a competition between homophily and homeostasis [6,7]. The adaptive evolution of the weights w_{ij}^l is governed by

$$\dot{w}_{ij}^l(t) = p_{ij}^l(t) - \left(\sum_{k \neq i} p_{ik}^l(t) \right) w_{ij}^l(t), \quad (3)$$

where the time dependent quantity $p_{ij}^l(t)$ is defined as

$$p_{ij}^l(t) = \frac{1}{T} \left| \int_{t-T}^{t} e^{i(\phi_i^l(t') - \phi_j^l(t'))} dt' \right|. \quad (4)$$

Notice that p_{ij}^l denotes, at time t, the average phase correlation (within layer l) between oscillators i and j over a characteristic memory time T. It follows from Eq. (3) that the normalization condition given by Eq. (2) holds at all times, i.e., the sum of the weights of all incoming connections at each node within each layer is conserved.

The particular case of a monoplex ($M = 1$) was extensively studied in Refs. [6,7], both numerically and analytically, and it was shown that a large region exists in the parameter space (σ_1, T) where, starting from random initial conditions for the weights w_{ij}^1 and phases ϕ_i^1, the network asymptotically reaches a state organized in synchronous clusters. Within this regime, the global phase coherence is rather small while the local coherence (i.e. the level of phase synchronization of each oscillator within its neighborhood) is very high, showing, at the same time, a scale-free distribution of the connection weights w_{ij}^1 as $t \to \infty$.

As we are here interested on investigating the competition between Hebbian learning and homeostasis in *multilayer* networks, we analyze the synchronization properties of the ensemble as a function of the two coupling parameters σ_1 and σ_2. In the following, and without loss of generality, we will fix $T = 100$, and concentrate on the analysis of the solution of Eqs. (1) and (3) for $N = 100$ oscillators and $M = 10$ layers. The purpose is understanding what the role of the interaction between layers is in the reorganization of the intra-layer structures. At this stage, several quantifying parameters need to be introduced and discussed. The first one is the classical time dependent order parameter [22]

$$r(t) = \frac{1}{MN}\left|\sum_{k=1}^{M}\sum_{j=1}^{N} e^{i\phi_j^k(t)}\right|, \tag{5}$$

which actually measures the level of global synchronization in the *whole* multilayer network.

In turn, the level of phase synchronization *within* a selected layer l can be quantified as

$$r^l(t) = \frac{1}{N}\left|\sum_{j=1}^{N} e^{i\phi_j^l(t)}\right|, \tag{6}$$

and, correspondingly, the degree of synchronization of the different phasors' components at each layer can be measured by averaging among all layers

$$r_{layers}(t) = \frac{1}{M}\sum_{k=1}^{M} r^k(t) = \frac{1}{MN}\sum_{k=1}^{M}\left|\sum_{j=1}^{N} e^{i\phi_j^k(t)}\right|. \tag{7}$$

Our first step is an extensive and careful numerical simulation of Eqs. (1) and (3) for inspecting how r and r_{layers} depend on the inter- and intra- layer coupling strengths, σ_1 and σ_2 respectively. A generic outcome is that, setting an initial all-to all coupling configuration for all layers and random initial conditions for the weights and for all the components of the phasors, an asymptotic state emerges spontaneously where all weights in the different layers take well-defined values. Specifically, we assign all links an initial (random) distribution of weights w_{ij}^l and phasors ϕ_i^l. Next, we let the whole network to evolve following Eq. (1) during $t_1 = 500$ time units, with all values of w_{ij}^l fixed at their initial conditions. After t_1, homophily and homeostasis are activated and the system follows Eqs. (1)–(4) during a time interval of $t_2 = 2,000$ time units. To guarantee that this second transient time t_2 is large enough for the network topology to attain its asymptotic state (except for negligible fluctuations) we calculate the quantity

$$\delta = \frac{1}{M}\sum_{l}^{M}\sqrt{\sum_{i,j}[w_{ij}^l(t) - w_{ij}^l(t-1)]^2} \tag{8}$$

and confirm that $\delta < 10^{-3}$ for all values of σ_1 and σ_2. Finally, all synchronization indicators are calculated along a further sufficiently long time interval τ after the transient t_2. Specifically, we average the values of r and r_{layers} during $\tau = 1,000$ time units and over $N_a = 10$ independent realizations, i.e.

$$r = \frac{1}{N_a\tau}\sum_{s=1}^{N_a}\int_{t_1+t_2}^{t_1+t_2+\tau} r_s(t)\,dt,$$

$$r_{layers} = \frac{1}{N_a\tau}\sum_{s=1}^{N_a}\int_{t_1+t_2}^{t_1+t_2+\tau} r_{layers_s}(t)\,dt. \tag{9}$$

Fig. 1 (a) and (b) report r and r_{layers} [calculated as specified in Eq. (9)] in the parameter space (σ_1, σ_2). As expected, the asymptotic value of r Fig. 1(a) depends on a nontrivial combination of σ_1 and σ_2. On the contrary, r_{layers} almost exclusively depends on σ_1 Fig. 1(b), as this order parameter accounts for the synchronization inside each layer. Nevertheless, it is worth noting the presence of

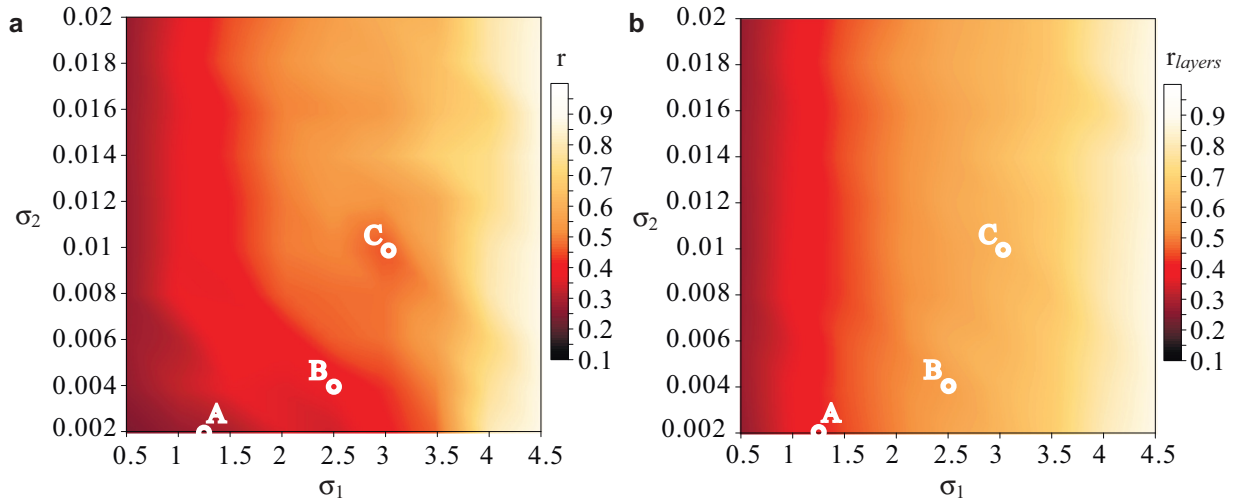

Fig. 1. Time averages of the global and layer synchronization indicators (a) r and (b) r_{layers} (see main text for definition) calculated in the (σ_1, σ_2) parameter space. Results refer to the asymptotic state ($\delta < 10^{-3}$, see main text for definition) obtained starting from random initial conditions for the weights w_{ij}^l (with the requirement of Eq. (2) being satisfied), and random initial phases ϕ_i^l selected uniformly in the interval $[-\pi, \pi]$. Each reported value corresponds to an average over 10 different initial conditions. The adaptation memory is $T = 100$. Points indicated as A, B and C will be discussed in Fig. 2.

several regions in the parameter space where the two parameters take remarkably different values. For instance, for $\sigma_1 = 2.5$ and $\sigma_2 = 0.004$, r_{layers} (∼0.6) is almost doubling the value of r (∼0.3), which indicates that the synchronization of the phasors within each layer is greater that in the whole multilayer network. The existence of moderate-to-high values of the parameter r is the consequence of the appearance of synchronized clusters, as already reported in the case of *monolayer* networks [6,7]. These clusters collapse into a unique large connected component when the coupling σ_1 is further increased. Nevertheless, once the multilayer structure is considered, the relation between r and r_{layers} gives additional information: it is indeed possible that the synchronized clusters differ from layer to layer. This is the case of moderate values of σ_1 and σ_2, which allow the phases ϕ_i^l of node i to evolve asynchronously between them while, at the same time, synchronizing in clusters at the different layers, thus leading to $r_{layers} > r$. When instead both σ_1 and σ_2 take large enough values, all phases within and between layers are in perfect synchrony, and $r_{layers} \sim r$.

The properties of the emergent dynamical state of the systems constitute only one side of the self-organization process. The fact that we are dealing with adaptive weights, indeed, makes the topology of the layers to evolve in time together with its own dynamics, up to reaching its emergent, asymptotic, configuration. To monitor the difference in the distribution of weights at each layer, we calculate the average of the difference of the weight coefficients w_{ij}^l between layers as

$$\Delta(t) = \frac{1}{M}\sum_{l=1}^{M}\sum_{i=1}^{N}\sum_{j=1}^{N}\sum_{k\neq l}\left|w_{ij}^l(t) - w_{ij}^k(t)\right|. \tag{10}$$

As in the case of the other parameters, Δ is averaged over $\tau = 1,000$ time units (after the asymptotic state is reached) and over $N_a = 10$ independent realizations:

$$\Delta = \frac{1}{N_a\tau}\sum_{s=1}^{N_a}\int_{t_1+t_2}^{t_1+t_2+\tau}\Delta_s(t)\,dt. \tag{11}$$

Fig. 2 illustrates the dependence of the quantity Δ on the coupling parameters σ_1 and σ_2. Dark regions correspond to values of the parameter Δ close to zero, indicating a perfect matching between the connection weights w_{ij}^l of all layers, i.e., $w_{ij}^l \approx w_{ij}^s$, $\forall l, s$. Combining large values of σ_1 and σ_2, indeed, leads to: (a) the same value of the phases ϕ_i on all layers of the network [see Fig. 1(a)], i.e., $\phi_i^l \approx \phi_i$, $\forall l$, and (b) the same topological structure for all layers [Fig. 2]. In this regime, all layers end up with identical structure, the multilayer nature of the network is lost, and the system behaves as an *effective monolayer network*.

Much more remarkably, there are certain regions of the parameter space where Δ is consistently higher than zero. Specifically, we identify three regions associated to three local maxima in the (σ_1, σ_2) phase space: A (1.25, 0.002), B (2.50, 0.004) and C (3.00, 0.01) [see Fig. 2 for details)].

For small values of the coupling strengths region surrounding A in Fig. 2, the absence of correlation of the weights is associated to synchronization parameters close to zero, both within and between layers see Fig. 1. Within this region, nodes' phases ϕ_i^l belonging to the same layer are not synchronized and, as a consequence, synchronous clusters of oscillators are not observed within layers nor between layers.

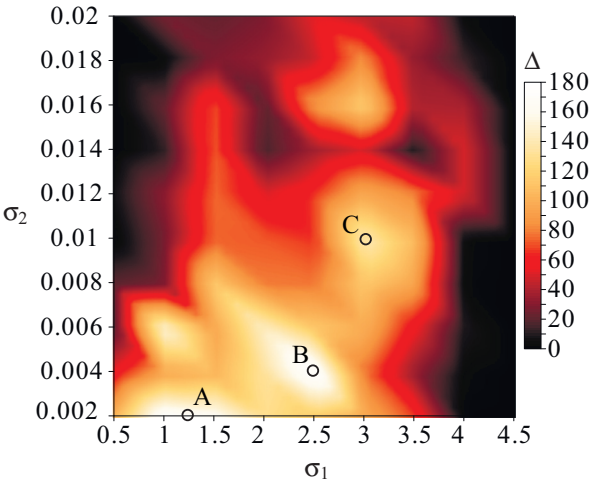

Fig. 2. Non-equivalence parameter Δ of the layer link topologies in the (σ_1, σ_2) parameter space. Local maxima are indicated as A, B and C (see main text for details). Same stipulations as in the caption of Fig. 1. Each reported value corresponds to an ensemble average over 10 different initial conditions.

In general, however, high values of Δ do not necessarily indicate that the final topologies of the layers are different. In Fig. 3 we show the probability distributions of the weights of the links after the adaptation process, for three particular layers $l = 1, 2, 3$ (similar distributions, not shown here, are obtained for the rest of the layers) and for the different regions around the local maxima of Δ. Fig. 3(a) shows the case where layers evolve independently (i.e., $\sigma_2 = 0$). We can observe that, despite there is no connection between layers, all of them evolve to similar distributions of weights. Adaptive monolayer networks with moderate couplings show similar weight distributions [7]. In Fig. 3(b) we plot instead the distributions obtained at the local maximum A. Once again one sees that, despite being uncorrelated (high Δ), the layers show again similar weight distributions.

A second region of interest surrounds the local maximum of Δ at point B = (2.5, 0.004), and it is characterized by sufficient difference between the value of r_{layer} ($r_{layer} >$ 0.6) and the value of r ($r < 0.45$) Fig. 1. The dynamical state of the system within this region is different from the previous one, since now synchronous clusters of oscillators start being formed at each layer, but, in general, these clusters are distinct from layer to layer, as indicated by the large value of Δ. Nevertheless, the averaged weight distributions $N(w_{ij}^l)$ for different layers Fig. 3(c) are still similar to the ones of Fig. 3(b).

The third area of interest surrounds the local maximum located at point C = (3.0, 0.01), and it is characterized by relatively high values both of r_{layer} ($r_{layer} \sim 0.5$) and r ($r \sim 0.65$). In this case, the phases of the oscillators evolve close to (but not yet in) the fully synchronized regime. Nevertheless, the fact that the oscillators are not

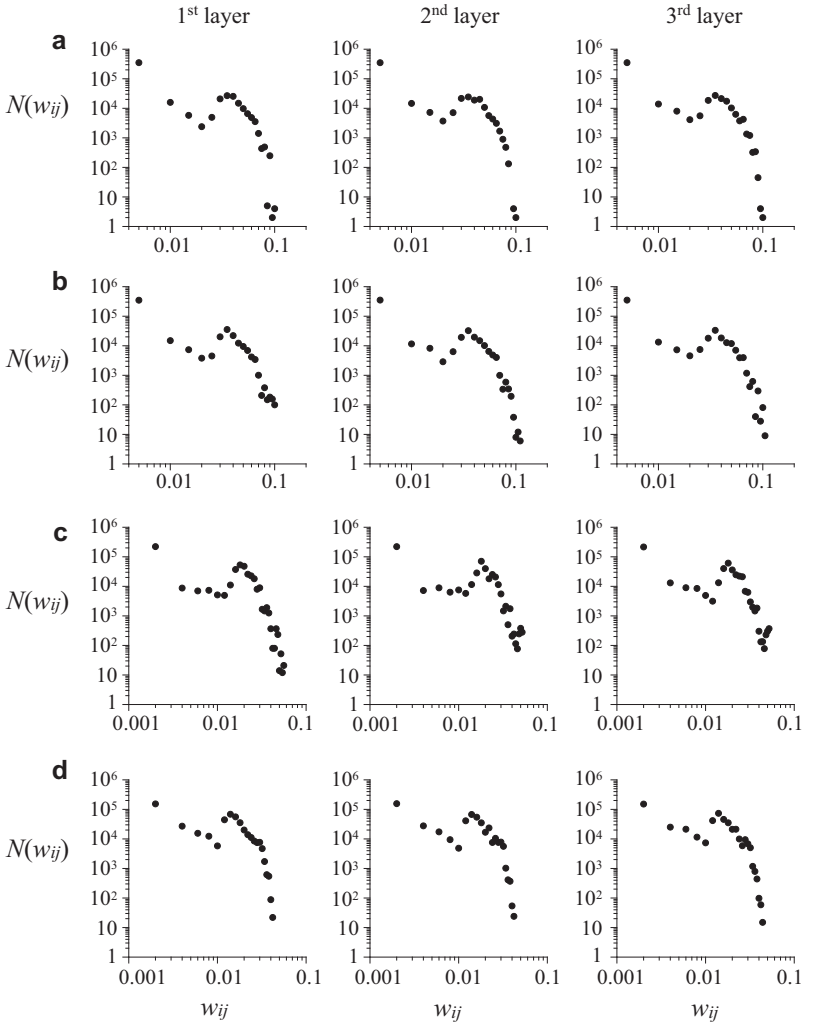

Fig. 3. Log-log plots of the weight distributions $N(w_{ij})$ at layer 1 (first column), 2 (second column) and 3 (third column), for different choices of the coupling parameters. Data obtained via $N_a = 50$ realizations: (a) $\sigma_1 = 1.25, \sigma_2 = 0.0$ (layers evolve independently from each other in this case), (b) $\sigma_1 = 1.25, \sigma_2 = 0.002$ (point A in Fig. 2), (c) $\sigma_1 = 2.5, \sigma_2 = 0.004$ (point B in Fig. 2), (d) $\sigma_1 = 3.0,\ \sigma_2 = 0.01$ (point C in Fig. 2). All other stipulations as in the caption of Fig. 1.

completely synchronized (since $r < 1$ and $r_{layers} < 1$) allows the layers to have uncorrelated weights, as indicated by $\Delta > 0$. As in the previous regions, the cumulative distribution of weights $N(w^l_{ij})$ of the different layers Fig. 3(c) do not differ substantially from layer to layer.

As an example to illustrate the impact of inter-layer strength on the formation of different clusters among the layers, we show in Fig. 4 the adjacency matrix of two layers for different inter-layer couplings (σ_2). In order to facilitate the identification of clusters inside each network we sorted the node number by its value in the second smallest eigenvector of the Laplacian matrix of the 1st layer [25]. We can see that at low inter-layer strengths Fig. 4(a) some of the communities at the layers are different. In fact, the general community structure is similar, but a number of nodes is assigned to different clusters, and some communities merge. If we quantify the differences between topologies using Eq. (10) for each pair of layers (instead of the whole multilayer structure) we obtain $\Delta_{1,2} = 39.43$. Increasing of the value σ_2 Fig. 4(b) results in a reduction of the difference between layer topologies ($\Delta_{1,2} = 21.52$), which can be observed directly at the adjacency matrices: now only two communities differ sufficiently. Finally, a further increase of σ_2 Fig. 4(c) leads to almost full overlap between layers ($\Delta_{1,2} = 1.03$), i.e. we obtain the same community structure inside each layer.

As a preliminary conclusion, we can affirm that different dynamical regimes lead to uncorrelated weights from layer to layer but, surprisingly, to similar probability distributions. This fact suggests that the cumulative distributions reported here in Fig. 3 (and, for monolayer networks, in Refs. [6,7]) are generic enough when homeostasis and homophily constrain the evolution of the network structure.

Finally, we analyzed the spectral properties of the emergent network, to discuss few dynamical properties of

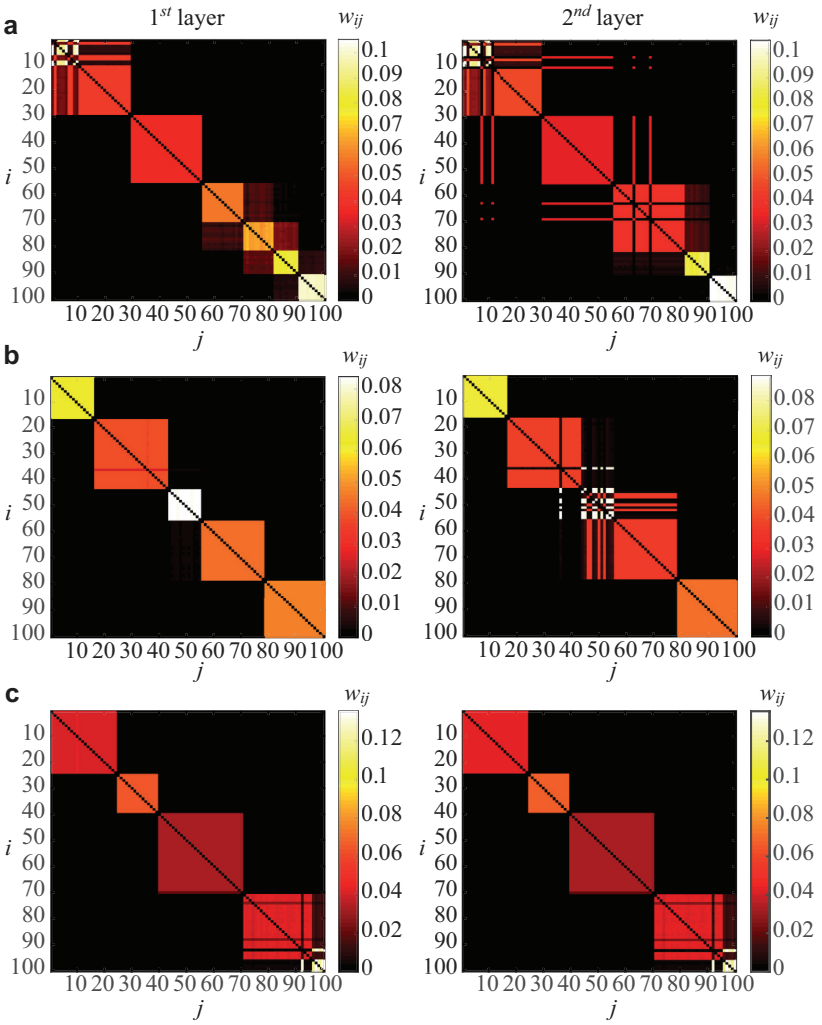

Fig. 4. Adjacency matrixes of 1st and 2nd layer, sorted by ranking of nodes at the 1st layer. Intra-layer coupling is $\sigma_1 = 1$ for all cases (a–c) and inter-layer coupling σ_2 is increased: (a) $\sigma_2 = 0.002$, (b) $\sigma_2 = 0.006$, (c) $\sigma_2 = 0.018$. Quantitative differences between layer topologies (see definition in the text): (a) $\Delta_{1,2} = 39.43$, (b) $\Delta_{1,2} = 21.52$, (b) $\Delta_{1,2} = 1.03$. In all cases, the adaptation memory is $T = 100$.

its final topology. To that purpose, we consider the network's weighted supra-Laplacian matrix. For the case of a monolayer network, the weighted Laplacian matrix is defined as $\mathcal{L} = \mathbf{S} - \mathbf{W}$, with $\mathbf{W}$ containing the weights of the network's links, and $\mathbf{S}$ being a diagonal matrix accounting for the strength of each node, defined as $s_{ii} = \sum_j w_{ij}$. In our case, the supra-Laplacian matrix $\mathcal{L}_\mathcal{M}$ is a $MN \times MN$ matrix defined as:

$$\mathcal{L}_\mathcal{M} = \begin{pmatrix} \mathcal{L}^{\mathbf{1}} + \mathbf{M}\mathbb{I} & -\mathbb{I} & \dots & -\mathbb{I} \\ -\mathbb{I} & \mathcal{L}^{\mathbf{2}} + M\mathbb{I} & \dots & -\mathbb{I} \\ \vdots & \vdots & \ddots & \vdots \\ -\mathbb{I} & -\mathbb{I} & \dots & \mathcal{L}^{\mathbf{M}} + M\mathbb{I} \end{pmatrix} \tag{12}$$

Where each diagonal block $\mathcal{L}^i$ accounts for the $(N \times N)$ Laplacian matrix of layer i, and $\mathbb{I}$ is the $N \times N$ identity matrix. We extract the set of eigenvalues of $\mathcal{L}_\mathcal{M}$, $\lambda_1 \leq \lambda_2 \leq \ldots \leq \lambda_M N$, and focus on how the smallest non-zero eigenvalue λ_2 (note that $\lambda_1 = 0$, as $\mathcal{L}_\mathcal{M}$ is a zero-row sum matrix) depends on the values of σ_1 and σ_2. From the point of view of the structural properties of the network, low values of λ_2, also known as the algebraic connectivity [26], are a signature of the modular structure of the network: a value of λ_2 close to zero indicates indeed that the network is close to be broken into isolated modules [25].

The values of λ_2 in the parameter space (σ_1, σ_2) are reported in Fig. 5, and one can clearly distinguish two main regions of interest: (a) a region where the values of λ_2 are low and remain almost constant (dark region of Fig. 5) and (b) a region where λ_2 increases with both σ_1 and σ_2 (colored region of Fig. 5). This way, low to moderate values of σ_1 and σ_2 lead, in turn, to low values of λ_2 (dark region), revealing that the final structure of the multiplex network is close to be separated into isolated modules. On the contrary, high values of both σ_1 and σ_2 result in an increase of λ_2 but only when a certain threshold of both couplings is crossed ($\sigma_1 > 2.50$ and $\sigma_2 > 0.005$).

It is worth remarking that λ_2 gives insightful information also for other dynamical processes such as diffusion

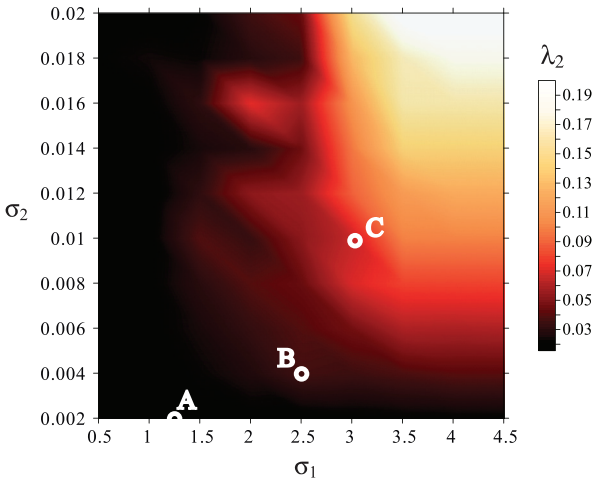

Fig. 5. Smallest non-zero eigenvalue λ_2 of the supra-Laplacian matrix (after the adaptation process is completed, see main text for details) as a function of the parameter space (σ_1, σ_2). The value of λ_2 is obtained after averaging over 10 independent realizations. [5]: the higher the value of λ_2, the lower the coupling strength required to achieve synchronization.

[27] or synchronization [28]. Specifically, λ_2 goes with the inverse of the time to reach the equilibrium in a diffusion process [27]. At the same time, when dealing with identical dynamical systems that are diffusively coupled, λ_2 is related to the ability of a network to achieve complete synchronization in the case of having class II systems (see [5] for a definition of class II systems and their synchronization properties). Therefore, the dark region of Fig. 5 is related to an organization of the network structure that would need long times to reach the equilibrium of a diffusion process, at least longer than those associated to the structures emerging within the colored region of the same figure. At the same time, the structures emerging inside the dark region have worse synchronization properties than those obtained within the coloured region. Comparing these results with those of Fig. 2 we can observe that, despite the combination of high values of σ_1 and σ_2 leads to the highest λ_2 (i.e., low diffusion time and high synchronizability), there are intermediate values of both couplings, such as those of point C, where a high λ_2 co-exists with two layers of different structures (see Fig. 2).

In summary, we have studied the emergence and self-organization of multiplex adaptive networks in the presence of homophilic and homeostasis processes. We have used an extension of the Kuramoto model in order to describe the evolution of oscillators whose dynamical state is contained in a M-dimensional phasor. When inter- and intra-layer coupling strengths are large enough, the system fully synchronizes at all layers. Under these circumstances, the final weight distribution of all layers is identical, and the overall structure collapses in a single monolayer network. At variance, the competition of the two adaptive mechanisms leads, for moderate coupling strengths, to the formation of synchronous clusters that may be either distinct or identical within the different layers. Finally, inspection on the second smallest eigenvalue of the supra-Laplacian matrix reveals the existence of certain multilayer structures emerging at moderate inter- and intra-layer coupling strengths which support shorter transient times to reach diffusion processes' steady states and, at the same time, a better synchronizability. This findings expand the understanding of the impact of homophily and homeostasis on the structure of multiplex networks and could be related to other dynamical process such as the improvement of information transfer [29,30]. Further studies investigating how to translate our results to more sophisticated models could give more insights about the emergence of multilayer structures in real systems.

Acknowledgments

This work was supported by MINECO (Spain) through projects FIS2011-25167 and FIS2013-41057, and Russian Foundation for Basic Research through project 15-02-00624. A.E.H. acknowledges support from the Ministry of Education and Science of the Russian Federation in the framework of the providing researches (Project 931). A.E.H., O.I.M., V.V.M. and V.A.M. thank also the Ministry of Education and Science of the Russian Federation (Projects 3.23.2014K and 1045).

References

[1] Strogatz SH. Exploring complex networks. Nature 2001;410:268–76.
[2] Barabasi A-L, Albert R. Statistical mechanics of complex networks. Rev Mod Phys 2002;74:47–97.
[3] Newman ME. The structure and function of complex networks. SIAM Rev 2003;45:167–256.
[4] Watts DJ. Small worlds: the dynamics of networks between order and randomness. Princeton: Princeton University Press; 1999.
[5] Boccaletti S, Latora V, Moreno V, Chavez M, Hwang D-U. Complex networks: structure and dynamics. Phys Rep 2006;424:175–308.
[6] Assenza S, Gutierrez R, Gomez-Gardenes J, Latora V, Boccaletti S. Emergence of structural patterns out of synchronization in networks with competitive interactions. Scientif Rep 2011;1(99):1–8.
[7] Gutierrez R, Amann A, Assenza S, Gomez-Gardenes J, Latora V, Boccaletti S. Emerging meso- and macroscales from synchronization of adaptive networks. Phys Rev Lett 2011;107:234103. http://dx.doi.org/10.1103/PhysRevLett.107.234103
[8] McPherson M, Smith-Lovin L, Cook JM. Birds of a feather: homophily in social networks. Annu Rev Sociol 2001;27:415–44.
[9] Hebb D. The organization of behavior. New York: Wiley; 1949.
[10] Turrigiano GG, Nelson SB. Homeostatic plasticity in the developing nervous system. Nat Rev Neurosci 2004;5:97–107.
[11] Dunbar R. Grooming, gossip, and the evolution of language. Harvard University Press; 1998.
[12] Kivela M, Arenas A, Barthelemy M, Gleeson J, Moreno Y, Porter M. Dynamical and spectral properties of complex networks. J Complex Netw 2014;2:203–71.
[13] Boccaletti S, Bianconi G, Criado R, del Genio CI, Gomez-Gardenes J, Romance M, et al. The structure and dynamics of multilayer networks. Phys Rep 2014;544:1–122.
[14] Battiston F, Nicosia V, V L. Successful strategies for competing networks. Phys Rev E 2014;89:032804.
[15] De Domenico M, Solé-Ribalta A, Cozzo E, Kivelä M, Moreno Y, Porter M, et al. Mathematical formulation of multilayer networks. Phys Rev X 2013;3:041022.
[16] Solá L, Romance M, Criado R, Flores J, del Amo AG, Boccaletti S. Eigenvector centrality of nodes in multiplex networks. Chaos 2013;23:033131.
[17] Min B, Yi S, Lee K-M, Goh K-I. Network robustness of multiplex networks with interlayer degree correlations. Phys Rev E 2014;89:042811.
[18] Sorrentino F. Synchronization of hypernetworks of coupled dynamical systems. New J Phys 2012;14:033035.
[19] Irving D, Sorrentino F. Synchronization of dynamical hypernetworks: dimensionality reduction through simultaneous block-diagonalization of matrices. Phys Rev E 2012;86:056102.

[20] Bogojeska A, Filiposka S, Mishkovski I, Kocarev L. Synchronization of dynamical hypernetworks: dimensionality reduction through simultaneous block-diagonalization of matrices. Telecommun Forum, TELFOR 2013;2013:172–5.
[21] Gutiérrez R, Nadal MSn, Zanin I, Papo D, Boccaletti S. Targeting the dynamics of complex networks. Sci Rep 2012;2:396.
[22] Kuramoto Y. Chemical oscillations, waves and turbulence. New York: Springer; 1984.
[23] Acebrón J, Bonilla L, Vicente C, Ritort F, Spigler R. The kuramoto model: a simple paradigm for synchronization phenomena. Rev Mod Phys 2005;77:137–85.
[24] Dörfler F, Bullo F. Synchronization in complex networks of phase oscillators: a survey. Automatica 2014;50:1539–64.
[25] Newman M. Finding community structure in networks using the eigenvectors of matrices. Phys Rev E 2006;74:036104.
[26] Fiedler M. Laplacian of graphs and algebraic connectivity. Combinat Graph Theory 1989;25:57–70.
[27] Radicchi F, Arenas A. Abrupt transition in the structural formation of interconnected networks. Nat Phys 2013;9:717–20.
[28] Aguirre J, Papo D, Buldú J. Successful strategies for competing networks. Nat Phys 2013;9:230–4.
[29] Mafahim JU, Lambert D, Zare M, Grigolini P. Complexity matching in neural networks. New J Phys 2015;17:015003.
[30] Pramukkul P, Svenkeson A, West B, Grigolini P. The value of conflict in stable social networks. EPL 2015;111:58003.